DOI: 10.21776/ub.jpacr.2022.011.03.703 *J. Pure App. Chem. Res.*, **2022**, 11 (3), 207-213
30 December 2022

Synthesis of $Bi_4Ti_3O_{12}$ and $Bi_4Ti_{2.95}V_{0.05}O_{12}$ Micro Sheets via NaCl-KCl Molten Salt Method

Anton Prasetyo[1*], Andy Nur Muhammad Guntur[1], Suci Noerfaiqotul Himmah[1], Nur Aini[1], Usman Ali Rouf[1], Abdul Aziz[2]

[1]Department of Chemistry, Faculty of Science and Technology, Universitas Islam Negeri Maulana Malik Ibrahim Malang, Malang, Indonesia, 65144
[2] Department of Mathematics, Faculty of Science and Technology, Universitas Islam Negeri Maulana Malik Ibrahim Malang, Malang, Indonesia, 65144

[*]Corresponding email: anton@kim.uin-malang.ac.id

Received 29 August 2022; Accepted 30 December 2022

ABSTRACT

$Bi_4Ti_3O_{12}$ is a tri-layer Aurivillius member compound that was reported to have good photocatalytic properties. Metal element doping and morphological particle tuning are strategies to increase photocatalyst activity. In this research, $Bi_4Ti_3O_{12}$ and $Bi_4Ti_{2.95}V_{0.05}O_{12}$ microsheets were synthesized using NaCl/KCl molten salt method. SEM and X-ray powder diffraction pattern of the products show that the $Bi_4Ti_3O_{12}$ and $Bi_4Ti_{2.95}V_{0.05}O_{12}$ microsheets were successfully synthesized. However, the $Bi_4Ti_{2.95}V_{0.05}O_{12}$ contains some impurities. UV-Vis DRS analysis of both samples resulting in a band gap energy of ~2.97 eV.

Keywords: $Bi_4Ti_3O_{12}$, $Bi_4Ti_{2.95}V_{0.05}O_{12}$, molten salt synthesis, NaCl-KCl, micro sheets.

INTRODUCTION

Dye waste have given negative impacts on the environment, so an efficient dye waste treatment is needed to maintain the sustainability of environment. One of the potential methods that have good ability in handling dye waste is photocatalyst technology [1, 2]. Several compounds have been reported to have the properties as photocatalyst materials, one of those materials is the Aurivillius structure compound [3, 4]. The general formula of Aurivillius compounds is $[Bi_2O_2]^{2+}[A_{m-1}B_mO_{3m+1}]^{2-}$ which is arranged alternately between bismuth and pseudo-perovskite layers. Cation-*A* is occupied by monovalent, divalent, or trivalent cations, such as Na^+, Ca^+, Sr^{2+}, Ba^{2+}, Pb^{2+}, or Bi^{3+}, while cation-*B* is occupied by high valence cations, such as Ti^{4+}, Nb^{5+}, or Ta^{5+}. The number of layers in Aurivillius is indicated by the number of pseudo perovskite layers denoted by "*m*" which is an integer number [5]. The advantage of Aurivillius compound as a photocatalyst material is caused by its ferroelectric properties that lead to reduce the rate of electron-holes recombination so that increasing photocatalytic activity [6]. In addition, the valence band of Aurivillius structure that involving electrons in the O 2*p* and Bi 6*s* orbitals is reported to increase photocatalytic activity [7].

The $Bi_4Ti_3O_{12}$ compound is classified as a tri-layers Aurivillius compound which has been reported to be potentially used as photocatalyst material with a band gap energy of 2.96 eV (419 nm) [8]. Meanwhile, some researchers reported that metal doping such as Fe or Cr on $Bi_4Ti_3O_{12}$ compounds can increase its visible light absorption [9, 10]. Therefore, the

$Bi_4Ti_3O_{12}$ photocatalyst can use a wider visible light range advantageously as an excitation source. The use of vanadium as metal doping on photocatalysts material has also been reported by several researchers. Li *et al*. (2020) have reported that the presence of vanadium doping on TiO_2 can reduce its band gap energy so it can work effectively under visible light [11]. It indicates that vanadium metal has the potency to be used in reducing the band gap energy of $Bi_4Ti_3O_{12}$.

The particle morphology of $Bi_4Ti_3O_{12}$ has been reported to have an influence on its photocatalytic activity. Previous research reported that the plate-like particle of $Bi_4Ti_3O_{12}$ has a good photocatalytic activity [12, 13]. In addition, Chen *et al*. (2016) state that $Bi_4Ti_3O_{12}$ with nanosheet morphology has a good ability to degrade rhodamine B due to the high number of actives sites on its surface which can inhibit the rate of electron (e^-)-hole (h^+) recombination [13]. It indicated that the sheet/plate-like $Bi_4Ti_3O_{12}$ can provide more advantageous properties as a photocatalyst compound.

The molten salt method (MSS) is one of the simplest methods that can produce a unique particle morphology. This method has several advantages including (a) cheap, (b) environmentally friendly, and (c) lower synthesis temperature compared to the solid-state reaction method [14]. The synthesis of $Bi_4Ti_3O_{12}$ using the MSS method has been reported by many researchers [15, 16]. Moreover, Liu *et al*. (2017) have reported that they have succeeded in synthesizing the Fe-doped $Bi_4Ti_3O_{12}$ compound using the MSS method and obtained a nanosheet morphology that has a good photocatalytic activity [18]. It indicates that the MSS method can be used in metal doped $Bi_4Ti_3O_{12}$ synthesis and obtained the nanosheet morphology that can increase its photocatalytic activity. Based on the description above, vanadium doped $Bi_4Ti_3O_{12}$ is studied and reported in this research, using the MSS method. The product phase, particle morphology, and band gap energy are also discussed.

EXPERIMENT

Chemicals and Instrumentation

Precursors used in the synthesis of $Bi_4Ti_3O_{12}$ and $Bi_4Ti_{2.95}V_{0.05}O_{12}$ were Bi_2O_3 (Himedia, 99.9%), TiO_2 (Sigma Aldrich, 99.9%), and V_2O_3 (Sigma Aldrich, 99.9%). Other materials used were supplied from Merck, namely KCl (99.5%), NaCl (99.5%), $AgNO_3$ (99.9%), and acetone.

The phase of synthesized compounds was identified using the powder *X*-ray diffraction (p-XRD) technique (Rigaku Miniflex diffractometer) with a measurement range of 2θ = 5 – 90°. The particle morphology was examined using scanning electron microscopy (SEM) (JEOL JSM-6360LA). The obtained micrographs were processed using Image-J software to determine the particle size. The reflectance spectrum was obtained from measurements using ultraviolet-visible diffuse reflectance spectroscopy (UV-Vis DRS) (Thermo Scientific Evolution 220 spectrometer type) with a measurement range of 200-800 nm. The DRS spectra were analyzed using the Kubelka-Munk equation to calculate the band gap energy.

Procedure synthesis

Three grams of the targeted compound was synthesized by NaCl-KCl (1:1) molten salt method with a molar ratio of the targeted compound and salt is 1:7. The precursors were weighed according to the stoichiometric calculations of the reaction. In the first stage, the precursors of Bi_2O_3, TiO_2, V_2O_3, and NaCl-KCl salt were grounded in a mortar agate for an hour, in which during the grinding step, the small amount of acetone was added to make a homogeneous mixture. Then, the mixture was calcined at temperatures of 750 and 850 °C for 6 hours. The product was washed using hot water to remove the salt. Identification of the

remaining NaCl-KCl salt was carried out by adding $AgNO_3$ solution into filtrate during the washing process. Finally, the sample was dried at 75 °C in an oven.

RESULT AND DISCUSSION

The product of $Bi_4Ti_3O_{12}$, and $Bi_4Ti_{2.95}V_{0.05}O_{12}$ are shown in Figure 1, in which the color of doped sample was changed due to the vanadium addition. The sample of $Bi_4Ti_3O_{14}$ compound had white color, while the vanadium doped sample produced slightly yellowish color which indicated a chemical change occurred after doping.

Figure 1. The sample of (a) $Bi_4Ti_3O_{12}$, and (b) $Bi_4Ti_{2.95}V_{0.05}O_{12}$

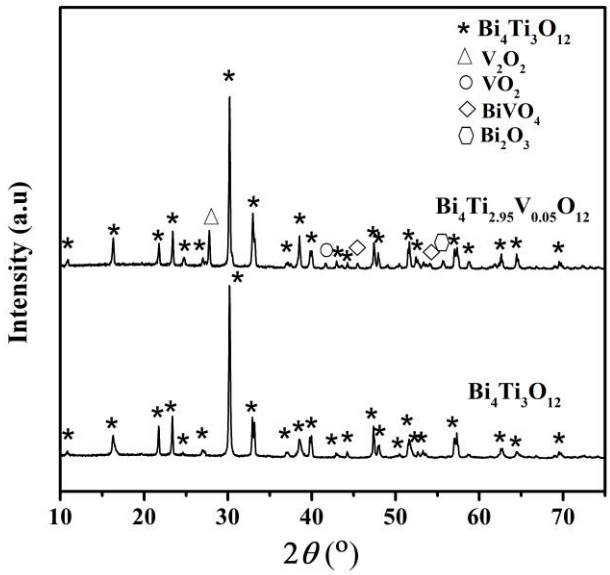

Figure 2. *X*-ray powder diffraction pattern of (a) $Bi_4Ti_3O_{12}$, and (b) $Bi_4Ti_{2.95}V_{0.05}O_{12}$

The *X*-ray powder diffraction pattern of sample of $Bi_4Ti_3O_{12}$, and (b) $Bi_4Ti_{2.95}V_{0.05}O_{12}$ are shown in Figure 2 and compared to that of the standard of $Bi_4Ti_3O_{12}$ from the Joint Committee on Powder Diffraction Standard (JCPDS) No. 35795. The comparison result showed that the $Bi_4Ti_3O_{12}$ and (b) $Bi_4Ti_{2.95}V_{0.05}O_{12}$ sample had conformity with the $Bi_4Ti_3O_{12}$ standard which was shown to have a typical diffraction peak at 2θ = 10.60, 16.20, 21.65, 23.14, 30.20, 32.80, 38.20, 47.18, 51.44, 57.08, 62.60, and 64.21°. The impurities in the $Bi_4Ti_{2.95}V_{0.05}O_{12}$ sample were identified as: (a) Bi_2O_3 which was identified by the presence of peak 43.62, and 55.62˚ (JCPDS No. 006-0312) (b) V_2O_2 which was identified by the presence of peak 27.76˚ (JCPDS No. 019-1398) (c) VO_2 with the presence of peak 41.67˚ (JCPDS No. 033-1440), and (d) $BiVO_4$ with peak 45.46˚ (JCPDS No. 01-074-1721). The presence of Bi_2O_3 impurity indicates that there is unreacted precursor mixed with the product. Meanwhile, V_2O_2, VO_2, and $BiVO_4$ impurities indicate that vanadium is difficult to replace

the position of the Ti atom in $Bi_4Ti_3O_{12}$ and tend to form different compound. Further look into the ionic radii of *B*-cation, the ionic radii of Ti^{4+} atom is 0.605 Å whereas the ionic radii of V^{3+} is 0.640 Å [19]. Since the difference is small, both cations may easily replace each other, theoretically. However, the position of highest intensity peak is relatively the same and impurities are also present. This suggest that the synthesis conditions remain unable to replace Ti^{4+} with V^{3+} at *B*-site.

The particle morphology of (a) $Bi_4Ti_3O_{12}$ and (b) $Bi_4Ti_{2.95}V_{0.05}O_{12}$ are shown in Figure 3 and it is observed that the particle morphology of the synthesis product was in the form of micro sheets, which is similar to work result that reported by Liu *et al*. (2017) [10]. However, the micro sheets produced in this study have a larger size. The results of the size calculation using the Image-J software are summarized in Table 1, which shows that the obtaining particles have a length and width in the range of 2.614 – 4.170 μm, while the thickness of selected particles is in the range of 0.224 – 0.407 μm. This large particle size indicates that the particle growth rate is greater than the nucleation rate or crystal seed formation [15, 17].

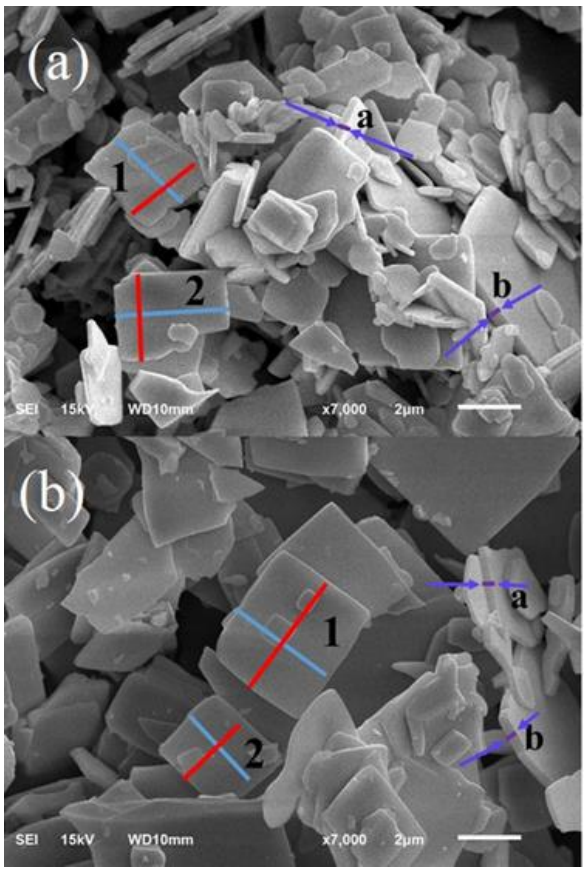

Figure 3. Particle morphology of (a) $Bi_4Ti_3O_{12}$, and (b) $Bi_4Ti_{2.95}V_{0.05}O_{12}$ (Red line denotes the length of particle; blue line indicates the width of particle and purple arrow denotes the thickness of particle)

Particle size calculated using the MSS method is also influenced by the composition of precursors because it affects the solubility of salt [14, 20]. Table 1 shows that the sample size of $Bi_4Ti_{2.95}V_{0.05}O_{12}$ is larger (length *x* width) than that of the $Bi_4Ti_3O_{12}$, which indicated that the presence of V_2O_3 precursors is affecting the particle growth. The direction of particle

growth is also different by comparing of sample thickness, in which the $Bi_4Ti_3O_{12}$ sample is thicker and indicates that the $Bi_4Ti_3O_{12}$ particle growth tend to be upward (vertical) while the $Bi_4Ti_{2.95}V_{0.05}O_{12}$ particle tend to grow horizontally.

Table 1 The particle size of (a) $Bi_4Ti_3O_{12}$, and (b) $Bi_4Ti_{2.95}V_{0.05}O_{12}$

Compound	Particle	Length (μm)	Width (μm)	Thickness (μm)
$Bi_4Ti_3O_{12}$	1	2.870	2.740	-
	2	3.550	2.773	-
	a	-	-	0.244
	b	-	-	0.407
$Bi_4Ti_{2.95}V_{0.05}O_{12}$	1	4.170	3.721	-
	2	3.028	2.614	-
	a			0.250
	b			0.339

Table 2. The band gap energy and absorption of (a) $Bi_4Ti_3O_{12}$, and (b) $Bi_4Ti_{2.95}V_{0.05}O_{12}$

Compound	Band gap energy (eV)
$Bi_4Ti_3O_{12}$	2.96
$Bi_4Ti_{2.95}V_{0.05}O_{12}$	2.97

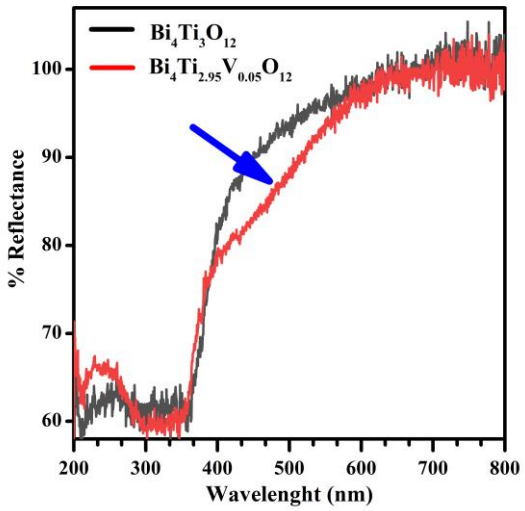

Figure 4. %Reflectance spectra of (a) $Bi_4Ti_3O_{12}$, and (b) $Bi_4Ti_{2.95}V_{0.05}O_{12}$

DRS spectra of $Bi_4Ti_3O_{12}$ and (b) $Bi_4Ti_{2.95}V_{0.05}O_{12}$ sample are shown in Figure 4, in which slightly shifted the reflectance to the visible light range was observed. It is indicating that the presence of vanadium influenced to reflectance spectrum. The DRS spectra were then analyzed using the Kubelka-Munk equation, in which the Tauc plot are shown in Figure 5. The results of the band gap energy are tabulated in Table 2. The band gap energy of $Bi_4Ti_3O_{12}$ compounds obtained in this work has similarity with previous work reported by Wang *et al.* (2020) [21]. Electronic transition that occurs in $Bi_4Ti_3O_{12}$ compounds involves

electrons in the O 2*p* and Bi 2*s* orbitals which are occupied the valance band and electrons in the Ti 3d orbitals of a conduction band [22]. The band gap energy of the $Bi_4Ti_{2.95}V_{0.05}O_{12}$ sample was slightly similar to that of $Bi_4Ti_3O_{12}$ sample and this correlate to the results of the *X*-ray powder diffraction pattern which suggest that the V^{3+} did not successfully replace the Ti^{4+}, hence new electronic transitions were not formed.

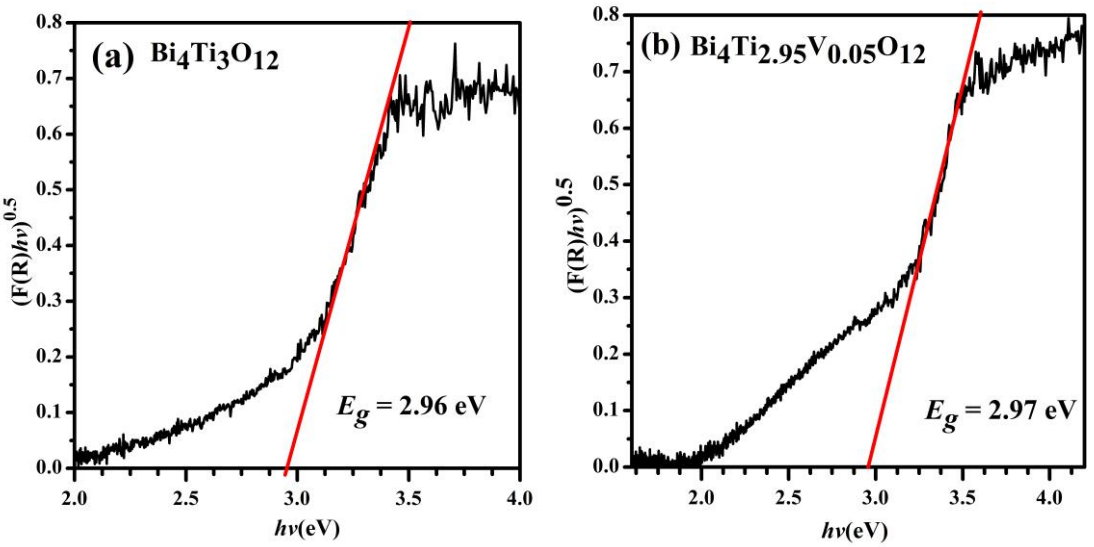

Figure 5. Tauc plot of (a) $Bi_4Ti_3O_{12}$, and (b) $Bi_4Ti_{2.95}V_{0.05}O_{12}$

CONCLUSION

The $Bi_4Ti_3O_{12}$ compound was successfully synthesized, meanwhile $Bi_4Ti_{2.95}V_{0.05}O_{12}$ did not formed. Impurities in $Bi_4Ti_{2.95}V_{0.05}O_{12}$ indicate that the vanadium has not been able to replace titanium significantly. The morphology of $Bi_4Ti_3O_{12}$ and $Bi_4Ti_{2.95}V_{0.05}O_{12}$ were in the form of micro sheets, in which the latter has a larger size than the former. In addition, the band gap energies of both compounds were considerably the same.

ACKNOWLEDGMENT

This research was funded by the 2020 BOPTN Research Grant Scheme, Institute for Research and Community Service (LP2M), Universitas Islam Negeri Maulana Malik Ibrahim Malang No DIPA BLU-DIPA 025.04.2.423812/2019.

REFERENCES

[1] Forgacs, E., Cserhati, T., and Orosb, G., *Environ. Int.*, **2004**, 30, 953–971.
[2] Anwer, H., Mahmood, A., Lee, J., Kim, K.H., Park, J.W., and Yip, A.C.K., *Nano Res.*, **2019**, 12, 5, 955-972.
[3] Zhu, Z., Wan, S., Zhao, Y., Gu, Y., Wang, Y., Qin, Y., Zhang, Z., Ge, X., Zhong, Q., and Bu, Y., *Materials Reports: Energy*, **2021**, 1, 100019.
[4] Rouf, U.A., Hastuti, E., and Prasetyo, A., *Jurnal Kartika Kimia*, **2021**, 4, 1, 51-57.
[5] Aurivillius, B. *Arkiv For Kemi*, **1949**, I, 54, 463-480.
[6] Khan, M. A., Nadeem, M. A. and Idriss, H., *Surf. Sci. Rep.*, **2016**, 71, 1, 1–31.
[7] Chen, P., Liu, H., Cui, W., Lee, S.C., Wang, L., and Dong, F., *EcoMat*, 2020, 2, 3, e12047
[8] Wang, Y., Zhang, X., Zhang, C., Li, R., Wang, Y., and Fan, C., *Inorg. Chem. Commun.*, **2020**, 116, 107931.

[9] Chen, Z., Jiang, X., Zhu, C., and Shi, C., *Appl. Catal. B.*, **2016**, 199, 241–251.
[10] Liu, Y., Zhu, G., Gao, J., Hojamberdiev, M., Zhu, R., Wei, X., Guo, Q., and Liu, P., *Appl. Catal. B.*, **2017**, 200, 72-82.
[11] Li, H., Zhao, G., Chen, Z., Han, G., and Song, B., *J. Colloid Interface Sci.*, **2010**, 344, 247–250.
[12] Zhao, W., Jia, Z., Lei, E., Wang, L., Li, Z., and Dai, Y., *J. Phys. Chem. Solids.*, **2013**, 74, 1604-1607.
[13] Chen, Z., Jiang, H., Jin, W., and Shi, C., *Appl. Catal. B.*, **2016**, 180, 698-706.
[14] Kimura, T. 2011, Molten salt synthesis of ceramic powders. *Advances in Ceramics Synthesis and Characterization, Processing and Specific Applications*. Rijeka: In Tech.
[15] Zhao, Z., Li, X., Ji, H., and Deng, M., *Integr. Ferroelectr.*, **2014**, 154, 54–158.
[16] Januari T., Aini N., Barorroh H., Prasetyo A., *IOP Conf. Ser.: Earth Environ. Sci*. 2020, 456: 012013.
[17] Marela, S.D., Aini, N., Hardian, A., Suendo, V., and Prasetyo, A., *J. Pure App. Chem. Res.*, **2021**, 10, 1, 64-71
[18] Liu, Y., Zhu, G., Gao, J., Hojamberdiev, M., Zhu, R., Wei, X., Guo, Q., and Liu, P., *Appl. Catal. B.*, **2017**, 200, 72-82.
[19] Shannon, R. D. 1976. *Acta Crystallogr.*, 1976, A32, 751-767.
[20] H. Maulidianingtiyas, A. D. Prasetiyo, F. Haikal, I. N. Cahyo, V. N. Istighfarini, and A. Prasetyo., *Alchemy Jurnal Penelitian Kimia*, **2021**, 17, 2, 211-218.
[21] Wang, Y., Zhang, X., Zhang, C., Li, R., Wang, Y., and Fan, C., *Inorg. Chem. Commun.*, 2020, 116, 107931.
[22] Lardhi, S., Noureldine, D., Harb, M., Ziani, A., Cavallo, L., and Takanabe, K., *J. Chem. Phys.*, **2016**, 144, 134702.